12

Neural Mechanisms of Catching: Translating Moving Target Information into Hand Interception Movement

Wolfgang Kruse, Nicholas L. Port, Daeyeol Lee, and
Apostolos P. Georgopoulos

12.1 Introduction

The neural mechanisms underlying the visuomotor coordination of arm movements have been intensely investigated over the past 20-odd years (Georgopoulos, 1990; Kalaska and Crammond, 1992; Caminiti et al., 1996; Schwartz, 1994b). Most of the tasks used have involved movement of the arm toward stationary targets. Because the visual information about the target in such tasks is static, consisting simply of the target's location in space, the key corresponding movement parameters are the direction and amplitude of the movement. In real life, however, the visual target may change location, involving a dynamic aspect of visuomotor coordination. Previous studies addressed this issue partially by shifting the target location at various times during the reaction or movement time (Georgopoulos et al., 1981, 1983). With respect to monkey behavior, it was found that the hand moved first toward the first target for a period of time and then changed direction to move toward the second target. The duration of the movement toward the first target was a linear function of the time for which the first target remained visible. This result indicated that the arm motor system was strongly coupled to the visual system, and faithfully followed the changes in the location of the target. Similar results were also obtained in human subjects (Soechting and Lacquaniti, 1983). With respect to the neural mechanisms involved, it was found that cell activity in the motor cortex (Georgopoulos et al., 1983) and parietal cortex (Kalaska et al., 1981) changed promptly after the target changed location, from a pattern appropriate for a movement toward the first target to a pattern appropriate for a movement toward the second. Indeed, the duration of the first cell response was a linear function of the duration of the first target. Thus a strong and orderly influence of the visual condition was exerted on the neuronal

activity in the motor and parietal cortex, and that influence was later reflected on the hand movement. The delay from shifting the target to the change of neuronal discharge patterns (from the first to the second pattern) was about 130 ms (see figure 10 in Georgopoulos et al., 1983). This value can be regarded as an estimate of the delay involved in the flow of information "on-line" from the visual to the arm motor system under behavioral conditions favoring a strong dependence of the latter on the former.

In the monkey studies discussed above, the visual target was stationary and the monkeys were trained to move toward it. Under these conditions, the target shift served as a dynamic probe of visuomotor coordination. When the hand catches a moving target, however, we have a very different case of visuomotor coordination. Obviously, the drastic difference lies in the motion of the stimulus. In addition, a richer set of task instructions is possible as well; for example, to catch the target as fast as possible or to catch it at a certain location (given a predetermined stimulus trajectory). Finally, a richer set of strategies by which the task can be accomplished becomes available; for example, when the target moves slowly and the task is to catch it at a certain location, the subject can wait and make a single catching movement, or can move incrementally toward the catching point by making a number of smaller movements. Experiments in both humans (Port et al., 1997; Lee at al., 1997) and monkeys (Port et al., 2001) showed that such different strategies can indeed be adopted. Results from single-cell recordings in behaving monkeys have been published (Port et al., 2001; Lee et al., 2001).

12.2 Methods

Animals

Two male rhesus monkeys (*Macaca mulatta*, 8–11 kg body weight; referred to as "monkeys 1 and 2") were used. Monkeys 1 and 2 used their right and left hands in performing the tasks, respectively, and recordings were made from the hemisphere contralateral to the performing arm. The motor cortex of monkey 1 was recorded from in two separate sessions. In the first session (1a), the monkey was allowed to make free eye movements, whereas, in the second (1b), it was required to fixate a stationary target during task performance. For monkey 2, there were no restrictions on eye movements. Care and treatment of the animals during all stages of the experiments conformed to the principles outlined in *Principles of Laboratory Animal Care* (NIH publication no. 86-23, revised 1995) and were approved by the relevant institutional review boards.

Apparatus

All visual stimuli were displayed on a 14-inch color computer monitor (Gateway 1020NI) located 57 cm away from the monkey at approximately eye level. The monitor was adjusted for a screen resolution of 640 horizontal and 480 vertical pixels, with a refresh rate of 60 Hz. Seated in a primate chair, the animals controlled the feedback cursor displayed on the monitor by moving a two-dimensional articulated arm on a horizontal planar working surface. The apparatus has been described previously (Georgopoulos et al., 1981). The monkeys grasped the distal end of the arm with their hand pronated while the other hand was comfortably restrained in a large acrylic tube. The position of the arm in x-y coordinates was digitally sampled at a rate of 100 Hz, and with a spatial resolution of 0.125 mm. The gain was set to one so that movement of the feedback cursor had a one-to-one correspondence with that of the arm. A personal computer was used for experimental control, visual presentation, and data collection.

Behavioral Task

In the interception task (figure 12.1), the stimulus (1) traveled in a straight line at 45° to the vertical from either lower corner of the computer monitor toward the interception point at 12 o'clock (two target motion directions),

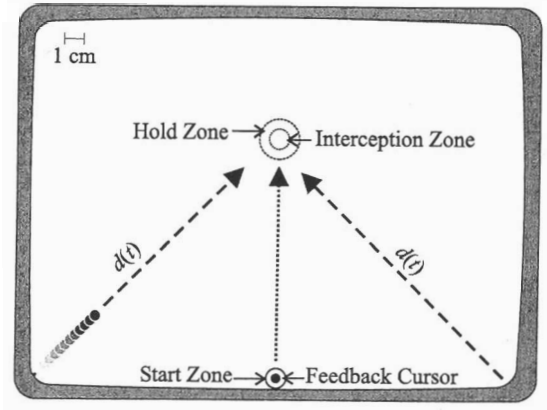

Figure 12.1
Spatial layout of the interception task.

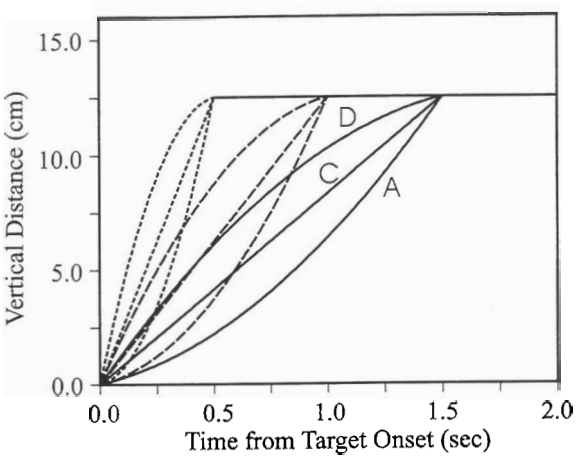

Figure 12.2
Temporal profile of stimuli used. (*Top*) Target displacement is plotted against time for all target motion times—0.5 s (dotted lines), 1.0 s (dashed lines), and 1.5 s (solid lines)—and target acceleration types (constant acceleration, constant deceleration, and constant velocity). A, C, D indicate accelerating, constant velocity, and decelerating targets, respectively.

(2) moved with constant velocity, constant acceleration, or constant deceleration (three target acceleration types), and (3) moved for a duration of 0.5 s, 1.0 s, and 1.5 s (three target motion times, or TMTs; figure 12.2). Eighteen classes of trials were generated by the combination of these three target parameters, and each combination was presented 2–3 times in a pseudo-random sequence. Accelerating targets had a starting velocity of 3.0 cm/s and underwent an appropriate constant acceleration to achieve the desired motion time. Decelerating targets had velocity profiles that were mirror images of those of the accelerating targets and underwent constant deceleration to end with a velocity of 3.0 cm/s. Constant-velocity targets traveled at the appropriate constant velocity to achieve the required motion time.

A trial in the task began when the monkey moved the feedback cursor (0.3 cm radius circle) into a start zone (1 cm radius circle for monkey 1; 0.5 cm radius circle for monkey 2) centered at the bottom of the screen along the vertical meridian (figure 12.1). After the monkey had maintained this position for a random period of 1–3 s (the start-hold period), a target (0.6 cm radius circle) appeared in the lower right or left corner of the screen. The target then traveled along a 45° path until it reached the vertical meridian of the screen, where it stopped at a location 12.5 cm directly above the center of the start zone. The monkey was required to move the feedback cursor to intercept the target just as it reached its final position at the center of the interception zone. This zone was an invisible positional window, namely, a 1.2 cm radius circle for monkey 1 and a 1.0 cm radius circle for monkey 2, centered on the final target location. The following conditions were required for a trial to be considered successful. First, the monkey had to maintain the cursor within the start zone until 130 ms after target onset. This condition was imposed to prevent anticipatory movements to the target. Second, the monkey had to move the arm so that the feedback cursor would enter the interception zone within 130 ms of the target's arrival at the interception point. And third, after the cursor entered the interception zone, the monkey had to maintain the cursor within an invisible, 2.0 cm radius, circular positional window (target-hold zone) for 0.5 s. Trials were aborted when any of the above listed conditions was violated. Monkeys were notified of unsuccessful trials with a tone, and rewarded for successful trials with a drop of juice. There were no other constraints on the animal's movements or their initiation.

Experimental Design

Eighteen combinations of two directions, three acceleration types, and three target motion times were presented in a randomized block design. In session 1a, two stimulus directions were nested within each combination of acceleration type and target motion times, and were presented in subblocks of 2–3 trials; in session 1b, two stimulus directions were completely randomized within a combination block. To obtain an equal number of successful trials for all target conditions, unsuccessful trials were rerandomized and repeated until correct performance was achieved.

Data Collection

Neural Recordings After an animal was trained to perform with greater than 85% accuracy in the task, recordings of cortical neurons during task performance were initiated using a seven-electrode recording system (Thomas RECORDING, Giessen, Germany; see Mountcastle et al., 1991; Lee et al., 1998). The electrophysiological techniques used to record the extracellular electrical signals of single-cell activity, the surgical procedures and the animal care have been described previously (Georgopoulos et al.,

1982; Lurito et al., 1991). All surgical procedures were performed under general anesthesia and aseptic conditions. A lightweight metal halo (Nakasawa Works Co., Tokyo, Japan) was used to stabilize the head during recording sessions. Neural impulses were discriminated on-line using dual-time-amplitude-window discriminators (BAK Electronics, Maryland) and computer-controlled spike template matching (Alpha Omega Engineering, Nazareth, Israel).

Eye Position Recordings For monkey 1, eye position was monitored by the sclera search coil method (CNC Engineering, Seattle); the coil was surgically implanted using the method of Judge and colleagues (1980). For monkey 2, eye position was monitored by an infrared oculometer (DR. BOUIS, Karlsruhe, Germany). Horizontal and vertical eye positions were sampled at 200 Hz. Once again, in recording from monkey 1 in session 1a and from monkey 2, there were no restrictions on eye movements; eye position data were collected throughout the trials. However, in recording from monkey 1 in session 1b, the animal was required to fixate within 2° of visual angle from the center of the start zone throughout the trials. A trial was aborted if visual fixation was broken at any time.

Histology After the experiments were completed, the area of recording was demarcated on the cortical surface with metal pins inserted at known recording locations using a microdrive placement system. The animal was then euthanatized with a lethal overdose of sodium pentobarbital, perfused transcardially with buffered formalin, fixed, and the brain removed for histological processing.

Data Analysis

General Standard statistical analyses (Snedecor and Cochran, 1989; Draper and Smith, 1981) were used, including multiple regression analysis. Ad hoc computer programs and commercially available statistical packages (SPSS, version 7, SPSS Inc., Chicago, 1996; BMDP/Dynamic, BMDP Statistical Software Inc., Los Angeles, 1993) were used for statistical analyses.

Analysis of Behavioral Data The hand position was smoothed and differentiated using the finite impulse response method (pass band 0–0.5 Hz; stop band 13–50 Hz).

Spike Density Function The spike train was converted to a spike density function for some analyses (MacPherson and Aldridge, 1979), calculated using the fixed kernel method (Richmond et al., 1987), with a Gaussian pulse width of 30 ms. Spike density functions were synchronized with target onset. Spike density functions of individual neurons were averaged to generate a population spike density function (figure 12.3A).

Multiple Linear Regression The nature of the interception task requires a tight temporal coupling between the motion of the stimulus and the movement of the hand. A multiple linear regression model was used to relate the population spike density function to the evolving position, velocity, and acceleration of the target and hand movement. The spike density at time t was expressed as a function of the position, velocity, and acceleration of the hand at time $t + \tau_H$, and the target at time $t + \tau_S$, where τ_H and τ_S were independent time shifts in relation to the spike density function (from −130 ms to +150 ms). A negative shift means that the movement of the hand or the movement of the target preceded the neural activity, and a positive shift means that the target or hand movement came after the neural activity. The following model was used:

$$PSDF_t = b_0 + b_1 d^S_{t+\tau_S} + b_2 \dot{d}^S_{t+\tau_S} + b_3 \ddot{d}^S_{t+\tau_S} + b_4 d^H_{t+\tau_H} + b_5 \dot{d}^H_{t+\tau_H} + b_6 \ddot{d}^H_{t+\tau_H} + \varepsilon_t$$

$$t + \tau \leq T,$$

where $PSDF$ is the population spike density function, d is displacement of the stimulus (S) or the hand (H) every 10 ms, $b_0, \ldots, b_6$ are regression coefficients, ε is an error term, τ_S, τ_H are time shifts for the stimulus and the hand, respectively (from −130 ms to +150 ms, in 10 ms intervals, see below), and T is the period of time from the onset of the target until the delivery of reward. The inequality above means that the neural data included within the shifted spike train were always contained within the behaviorally meaningful time period T. The shifting operation is illustrated in figure 12.3. To independently assess time shifts of the hand and of the target, two time shifts were used. For every time shift, the standardized regression coefficients (obtained from the raw regression coefficients by expressing them in standard deviation units, thus dimensionless) were also calculated. These coefficients allow researchers to compare the effects among the independent variables and provide information about

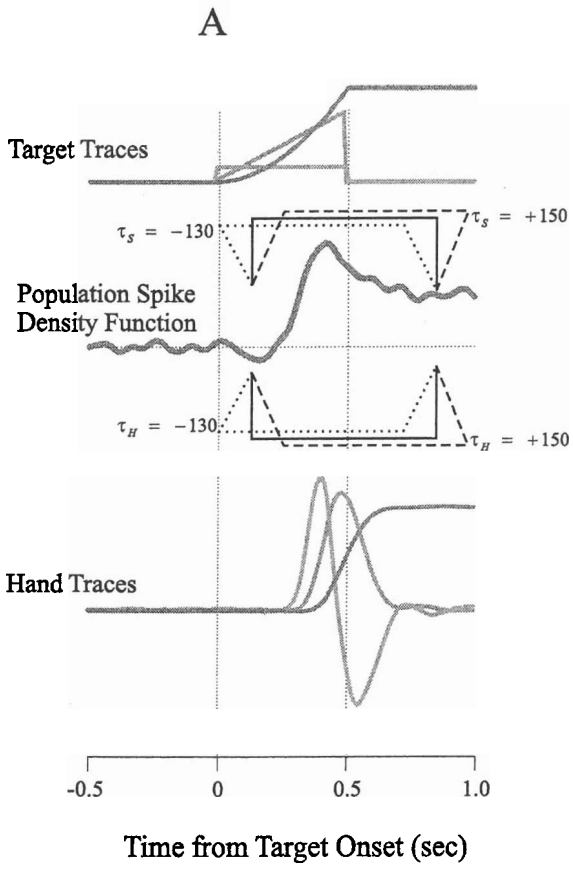

Figure 12.3
(*A*) Diagram of the multiple linear regression model (data from recording session 1a; accelerating target condition; target motion time 0.5 s). (*B, C*) Contour plots of the R^2 for all possible shifts (τ_S, τ_H) of the multiple linear regression model for recording sessions 1a and 1b, respectively.

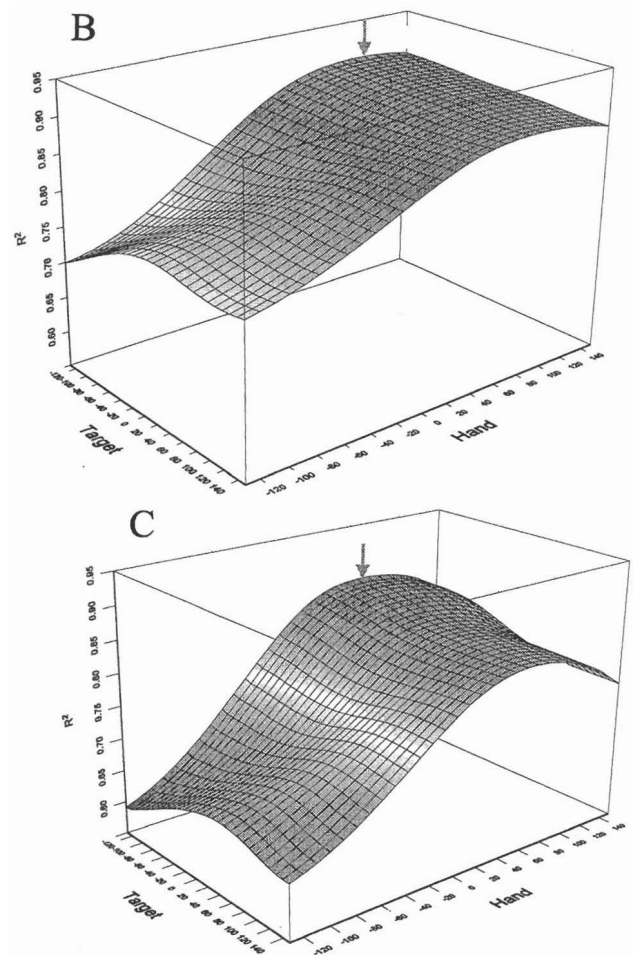

Figure 12.3 (*continued*)

the importance of a given variable in the regression equation. The coefficient of determination, R^2 (proportion of variance explained), was measured at all combinations of shifts, and the shift for which the highest R^2 was obtained, noted. The t statistic and its probability level were calculated for each coefficient. Because six simultaneous comparisons were performed, the nominal probability level was adjusted according to the Bonferroni inequality (Snedecor and Cochran, 1989) to $\alpha' = 0.05/6 \approx 0.008$; therefore, $P < .008$ was considered statistically significant. Finally, all regression analyses were run using default tolerance limits for collinearities among the independent variables; in none of the analyses were these default limits exceeded.

12.3 Results

A population spike density function from 407, 197, and 467 neurons was computed from recording sessions 1a, 1b, and 2, respectively. For some target conditions there was an early rise in the population spike density function even though the movement did not occur until several hundred milliseconds later (Port et al., 2001). At the best time shift, all coefficients in the model were significant with the exception of target acceleration in recording session 1b. The R^2 was calculated for each 10 ms shift. The results obtained are shown in table 12.1, which shows the R^2, best time shifts, and the standardized coefficients at the best time shift for each recording session. The relative importance of a particular variable on the population spike density function can be assessed by ranking the standardized coefficients. The rank-ordered standardized coefficients are listed in table 12.2. As is evident in these two tables, hand speed was generally the strongest explanatory variable for the population spike density function, followed closely by hand position and target position. Target velocity was generally fourth in the list, while hand and target acceleration had the weakest relation to the population spike density function. It is worth noting that the shifts of the target (−130 ms), t_2, are at their earliest. Shifts could not be made beyond these values due to the early onset of neural activity (130 ms for all recording sessions). The percent of variance explained (R^2) differed for different combinations of target and hand shifts. Two examples are illustrated in figure 12.3B–C, which give the R^2 values for all these combinations in recording sessions 1a and 1b, respectively. The highest R^2 (0.89, 0.86, and 0.75, for recordings 1a, 1b, and 2, respectively) were obtained

Table 12.1
R^2 and standardized coefficients of the regression model at best time shift

Recording session	Hand t_1	Target t_2	R^2	Hand			Target		
				Position	Velocity	Acceleration	Position	Velocity	Acceleration
1a	100	−130	.89	0.27	0.61	0.06	0.34	0.18	−0.08
1b	70	−130	.86	0.25	0.71	0.09	0.16	0.25	0.01*
2	50	−80	.75	−1.4	0.57	0.07	1.33	−0.08	0.07

* Coefficient was not significant.

Table 12.2
Rank order of the standardized coefficients

Order	Session 1a	Session 1b	Session 2
1	Hand velocity	Hand velocity	Hand position
2	Target position	Target velocity	Target position
3	Hand position	Hand position	Hand velocity
4	Target velocity	Target position	Target velocity
5	Target acceleration	Hand acceleration	Target acceleration
6	Hand acceleration	—*	Hand acceleration

* Coefficient was not significant.

at time shifts $(\tau_S, \tau_H) = (-130, +100)$, $(-130, +70)$, and $(-80, +50)$ (see table 12.1). The time shift results indicated, for all recordings, (1) that the time varying population spike density function dynamically predicted the time varying aspects of hand movement, and (2) that there was a feedforward dynamic effect of target velocity and position on the spike density function.

As can be seen in figure 12.3B–C, the effect of the target shift was relatively flat in comparison to the shift of the hand. To test whether there was a significant effect of the target shift, a linear regression by groups (BMDP/Dynamic program 1R; see "Data Analysis" in section 12.2) was performed (this directly tests whether the regression equations for different groups differ significantly). For the optimal shift of the hand, tests were performed to identify at what point away from the best target shift the equations differed significantly. There was no difference in the regression equation for the following target shifts: −130 ms to −90 ms in recording session 1a, −130 ms to −80 ms in session 1b, and −80 ms to −20 ms in recording session 2. For target shifts greater than these, there was a statistical difference in the regression equation. Because all of the ranges listed above are negative, it may be inferred that target motion exerted a consistent feedforward effect on neural activity.

12.4 Discussion

Our results document for the first time the dynamic forward flow of information, from moving target to motor cortex to hand movement. The lags found, based on optimal time shifts in the regression analysis, were well within the range of estimates of such effects from previous neurophysiological studies. For example, the delay of visual effects on motor cortical cell activity was estimated at about 130 ms in a target shift task (Georgopoulos et al., 1983). On the other hand, an optimal time lag of about 90 ms has been found in single-cell studies during reaching movements to stationary targets; at this value, the regression model between cell activity and movement parameters attained the highest R^2 (Ashe and Georgopoulos, 1994). Although neither the exact pathways nor the sequence of events for this information flow are known, it is obvious that they involve a number of areas intercalated between the visual inflow and motor cortical outflow, where both anatomical and physiological studies (Caminiti et al., 1996; Schwartz, 1994b) have implicated parietofrontal pathways, and between the motor cortex and motoneuronal activation, and where corticocortical interactions as well as subcortical loops are apparently involved. Thus large circuits participate in this visuomotor coordination; our results provide an experimental estimate of the overall delays. Finally, it should be noted that these estimates may depend on the paradigm used in this study: Other estimates may well be obtained using different paradigms. For example, Schwartz (1994a) found the lag between the population vector and arm movement decreased as the movement curvature decreased in a tracing task. Moreover, predictive smooth tracking is usually done at minimal or zero lags between the stimulus and the movement. It is interesting that the optimal target population lag was smaller in session 2 (range: −80 ms to −20 ms) than in session 1a (−130 ms to −90 ms) or 1b (−130 ms to −80 ms), a finding that probably reflects monkey 2's using a strategy that resembled tracking (see Port et al., 2001), where one would expect a close temporal, on-line coupling between the moving stimulus and movement-related neural activity. It is also noteworthy that the optimal target population lags were very similar for sessions 1a and 1b, which differed with respect to the presence (session 1b) or absence (session 1a) of fixation requirement. This finding is in accord with monkey 1's adopting the same strategy, namely, making mostly a single precise interception movement in both conditions (Port et al., 2001). The longer lags observed in this case are close to those found following a shift of stationary targets (Georgopoulos et al., 1983).

Finally, with respect to the parameters influencing motor cortical population activity, we found that, first, hand movement effects ranked consis-

tently higher than those of stimulus motion; and second, that the effect of acceleration of either hand or stimulus ranked lowest. These results are in keeping with those of previous studies regarding hand movement effects (e.g., Ashe and Georgopoulos, 1994) and underscore the importance of hand velocity and position as the key parameters for the information flow in the primary motor cortex.

Acknowledgments

The work reported in this chapter was funded by U. S. Public Health Service grant PSMH48185, the U.S. Department of Veterans Affairs, and the American Legion Brain Sciences Chair.

References

Ashe, J., and Georgopoulos, A. P. (1994). Movement parameters and neural activity in motor cortex and area 5. *Cereb. Cortex* 4: 590–600.

Caminiti, R., Ferraina, S., and Johnson, P. B. (1996). The sources of visual information to the primate frontal lobe: A novel role for the superior parietal lobule. *Cereb. Cortex* 6: 319–328.

Draper, N. R., and Smith, H. (1981). *Applied Regression Analysis*. New York: Wiley.

Georgopoulos, A. P. (1990). Eye-hand coordination and visual control of reaching: Studies in behaving animals. In *Comparative Perception*. Vol. 1, *Basic Mechanisms*, M. A. Berkley and W. C. Stebbins (eds.). New York: Wiley, pp. 375–403.

Georgopoulos, A. P., Kalaska, J. F., and Massey, J. T. (1981). Spatial trajectories and reaction times of aimed movements: Effects of practice, uncertainty and change in target location. *J. Neurophysiol.* 46: 725–743.

Georgopoulos, A. P., Kalaska, J. F., Caminiti, R., and Massey, J. T. (1982). On the relations between the direction of two-dimensional arm movements and cell discharge in primate motor cortex. *J. Neurosci.* 2: 1527–1537.

Georgopoulos, A. P., Kalaska, J. F., Caminiti, R., and Massey, J. T. (1983). Interruption of motor cortical discharge subserving aimed arm movements. *Exp. Brain Res.* 49: 327–340.

Judge, S. J., Richmond, B. J., and Chu, F. C. (1980). Implantation of magnetic search coils for measurement of eye position: An improved method. *Vision Res.* 20: 535–538.

Kalaska, J. F., and Crammond, D. J. (1992). Cerebral cortical mechanisms of reaching movements. *Science* 255: 1517–1523.

Kalaska, J. F., Caminiti, R., and Georgopoulos, A. P. (1981). Cortical mechanisms of two-dimensional aimed arm movements: 3. Relations of parietal (areas 5 and 2) neuronal activity to direction of movement and change in target location. *Soc. Neurosci. Abstr.* 7: 563.

Lee, D., Port, N. L., and Georgopoulos, A. P. (1997). Manual interception of moving targets: 2. On-line control of overlapping submovements. *Exp. Brain Res.* 116: 421–433.

Lee, D., Port, N. L., Kruse, W., and Georgopoulos, A. P. (1998). Neuronal population coding: Multielectrode recordings in primate cerebral cortex. In *Neuronal Ensembles: Strategies for Recording and Decoding*, H. Eichenbaum and J. Davis (eds.). New York: Wiley, pp. 117–136.

Lee, D., Port, N. L., Kruse, W., and Georgopoulos, A. P. (2001). Neuronal clusters in the primate motor cortex during interception of moving targets. *J. Cogn. Neurosci.* 13: 319–331.

Lurito, J. T., Georgakopoulos, T., and Georgopoulos, A. P. (1991). Cognitive spatial-motor processes: 7. The making of movements at an angle from a stimulus direction: Studies of motor cortical activity at the single-cell and population levels. *Exp. Brain Res.* 87: 562–580.

MacPherson, J. M., and Aldridge, J. W. (1979). A quantitative method of computer analysis of spike train data collected from behaving animals. *Brain Res.* 175: 183–187.

Mountcastle, V. B., Reitboeck, H. J., Poggio, G. F., and Steinmetz, M. A. (1991). Adaptation of the Reitboeck method of multiple microelectrode recording to the neocortex of the waking monkey. *J. Neurosci. Methods* 36: 77–84.

Port, N. L., Lee, D., Dassonville, P., and Georgopoulos, A. P. (1997). Manual interception of moving targets: 1. Performance and movement initiation. *Exp. Brain Res.* 116: 406–420.

Port, N. L., Kruse, W., Lee, D., and Georgopoulos, A. P. (2001). Motor cortical activity during interception of moving targets. *J. Cogn. Neurosci.* 13: 306–318.

Richmond, B. J., Optican, L. M., Podell, M., and Spitzer, H. (1987). Temporal encoding of two-dimensional patterns by single units in primate inferior temporal cortex: 1. Response characteristics. *J. Neurophysiol.* 57: 132–146.

Schwartz, A. B. (1994a). Direct cortical representation of drawing. *Science* 265: 540–542.

Schwartz, A. B. (1994b). Distributed motor processing in cerebral cortex. *Curr. Opin. Neurobiol.* 4: 840–846.

Snedecor, G. W., and Cochran, W. G. (1989). *Statistical Methods*. Ames: Iowa State University Press.

Soechting, J. F., and Lacquaniti, F. (1983). Modification of trajectory of a pointing movement in response to a change in target location. *J. Neurophysiol.* 49: 548–564.